

SUBTHERMAL FISSION CROSS-SECTION MEASUREMENTS FOR ^{233}U , ^{235}U AND ^{239}Pu

C. Wagemans*, P. Schillebeeckx, A.J. Deruytter and R. Barthélemy

Commission of the European Communities, Joint Research Centre - Geel-Establishment,
Central Bureau for Nuclear Measurements, 2440 Geel, Belgium.

Abstract: The ^{233}U , ^{235}U and $^{239}\text{Pu}(n,f)$ cross sections have been measured at GELINA down to 2 meV neutron energy using a liquid nitrogen cooled methane moderator. The neutron flux has been determined via the $^6\text{Li}(n,\alpha)t$ reaction. These measurements considerably enlarge the data base in the subthermal region, resulting in more reliable values for the Westcott g_f -factor and its temperature dependency. These new $\sigma_f(E)$ -data have also been used to calculate selected fission integrals.

(^{233}U , ^{235}U , ^{239}Pu , fission cross-section, range 0.002-20 eV)

Introduction

At the International Conference on Nuclear Data for Science and Technology in Antwerp (1982), Bouchard et al.¹ drew the attention to a discrepancy existing between the calculated temperature coefficient of reactivity for light water reactors and measured values obtained in integral experiments. In order to remove this discrepancy, Santamarina et al.² proposed that the energy dependence of certain differential nuclear data in the subthermal neutron energy region be modified with respect to the ENDF-B5 data file within their uncertainties. One of the quantities concerned was the shape of the $^{235}\text{U}(n,f)$ cross-section. Since also for the other common fissile nuclides the σ_f -data base in the subthermal neutron energy region appeared to be rather poor, which has a direct impact on the accuracy of the Westcott g_f -factor, a measurement campaign has been undertaken for these nuclides.

In the present paper, the results obtained for ^{233}U , ^{235}U and ^{239}Pu are reported and discussed.

Experimental Conditions

In order to perform these experiments under decent experimental conditions, a liquid nitrogen (77 °K) cooled methane moderator has been installed at GELINA (Geel Electron Linear Accelerator), which yields about five times more neutrons below 20 meV compared to the usual water-beryllium moderator at room temperature (fig.1).

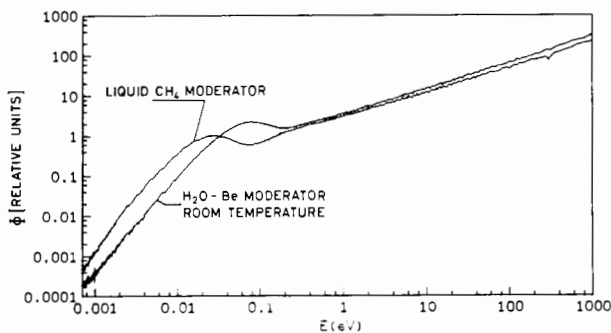


Fig. 1 Moderated neutron energy distribution at GELINA.

* NFWO, Univ. of Ghent and SCK/CEN, Mol, Belgium

The measurements were performed at a well-collimated 8.2 m flight-path of GELINA. The accelerator was operated at a 40 Hz repetition frequency with 2 μs burst widths and with an average electron current of 15 μA . An evaporated layer of 25 μg $^6\text{LiF}/\text{cm}^2$ used for the neutron flux determination and a fissile layer were mounted back-to-back in the center of a vacuum chamber with 50 cm diameter. The $^6\text{Li}(n,\alpha)t$ -particles and the fission fragments were detected in a low geometry with two 20 cm^2 large surface barrier detectors placed outside the neutron beam. After amplification and digitizing, the bi-dimensional pulse-height versus time-of-flight spectra were stored in a HP 1000 - A700 data acquisition system. The clean detection conditions are illustrated in fig. 2, which shows the $^6\text{Li}(n,\alpha)t$ and the $^{233}\text{U}(n,f)$ pulse-height spectra integrated over all t.o.f.-channels.

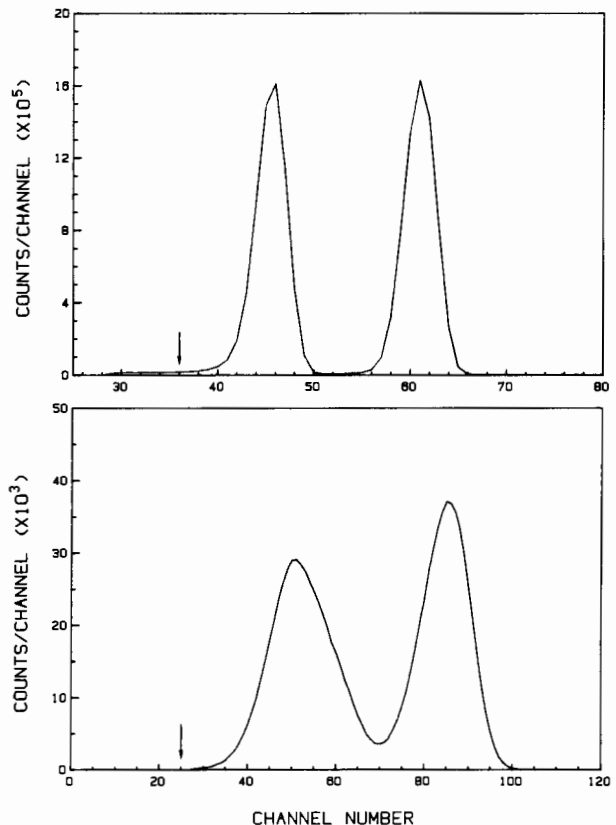


Fig.2 $^6\text{Li}(n,\alpha)t$ (upper curve) and $^{233}\text{U}(n,f)$ (lower curve) pulse-height spectra. The arrows indicate the discriminator settings used.

The thicknesses of the layers were chosen in such a way that absorption and self-absorption effects were very small. Homogeneously evaporated layers with the following thicknesses were used: 40 μg $^{233}\text{U}/\text{cm}^2$ ($^{233}\text{UF}_4$); 40 μg $^{235}\text{U}/\text{cm}^2$ ($^{235}\text{UF}_4$) and 30 μg $^{239}\text{Pu}/\text{cm}^2$ ($^{239}\text{PuF}_3$).

The neutron energy scale in the meV-region was verified by means of the prominent Bragg-reflection cuts in Be at 5.24 and 6.84 meV (fig. 3). The background was determined using the black resonances of Cd, Rh, Au and W. The background due to neutrons from overlapping bursts was checked by operating GELINA at 20 Hz.

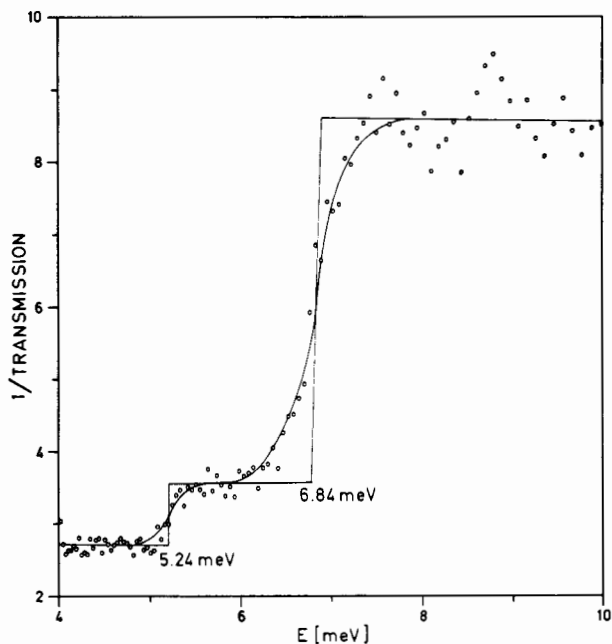


Fig. 3 Verification of the neutron energy scale with the Bragg-reflection cuts in Be.

Fig. 4 shows a typical example of a background curve determined via a polynomial fit through the black resonances. In fig. 5 the total $^{235}\text{U}(n,f)$ and $^6\text{Li}(n,\alpha)t$ counting-rate spectra are shown with the corresponding normalized background curves (lower full lines).

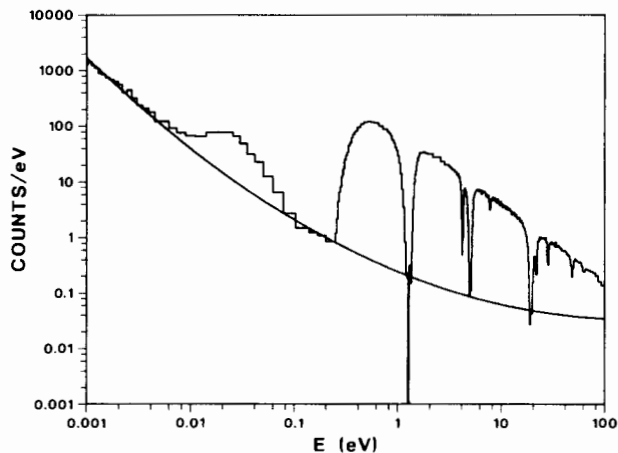


Fig. 4 Example of a polynomial fit through the black resonances.

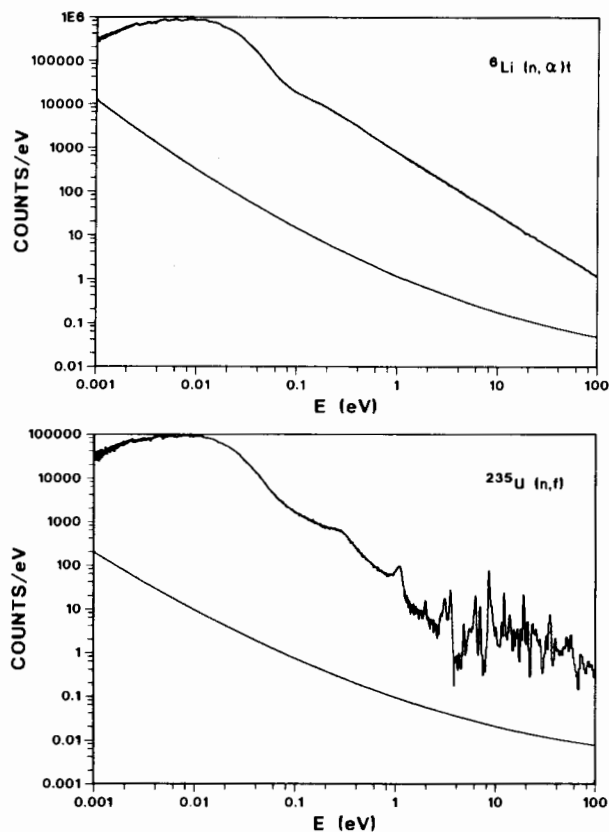


Fig. 5 $^6\text{Li}(n,\alpha)t$ and $^{235}\text{U}(n,f)$ counting rate spectra with the corresponding normalized background curves (lower full lines).

Results

Fission Cross-Section Measurements

All measurements were performed relative to the $^6\text{Li}(n,\alpha)t$ reaction, for which a $1/v$ shape was adopted in the energy region below 20 eV. In the case of ^{235}U , two measurements were performed, the first of which was reported³ at the Santa Fé Conference on Nuclear Data for Basic and Applied Science. For ^{233}U and for ^{239}Pu as well, only one experimental campaign has been performed.

The data reduction was done at the IBM 4381 using the APL-language and the ANGELA-routine⁴. The ratio of the background-corrected fission and ($\alpha + t$) counting-rates yields the $\sigma_f(E)\sqrt{E}$ shape, which still needs to be normalized. This normalization was done in the thermal region relative to the σ_f^0 -values proposed⁵ for the ENDF-B6 file, i.e.: 531.14 b ($\pm 0.25\%$) for ^{233}U , 584.25 b ($\pm 0.19\%$) for ^{235}U and 748.0 b ($\pm 0.25\%$) for ^{239}Pu , via the fission integrals

$$I_1 = \int_{0.020 \text{ eV}}^{0.050 \text{ eV}} \sigma_f(E) dE = (13.86 \pm 0.07) \text{ b.eV}$$

$$I_2 = \int_{0.02060 \text{ eV}}^{0.06239 \text{ eV}} \sigma_f(E) dE = (19.15 \pm 0.08) \text{ b.eV}$$

$$I_3 = \int_{0.0230 \text{ eV}}^{0.0600 \text{ eV}} \sigma_f(E) dE = (22.96 \pm 0.13) \text{ b.eV}$$

for ^{233}U ⁶, ^{235}U ⁷ and ^{239}Pu ⁸ respectively.

This normalization procedure was cross-checked by a polynomial fit through the normalized $\sigma_f(E)\sqrt{E}$ -data in the thermal region, yielding consistent σ_f° -values.

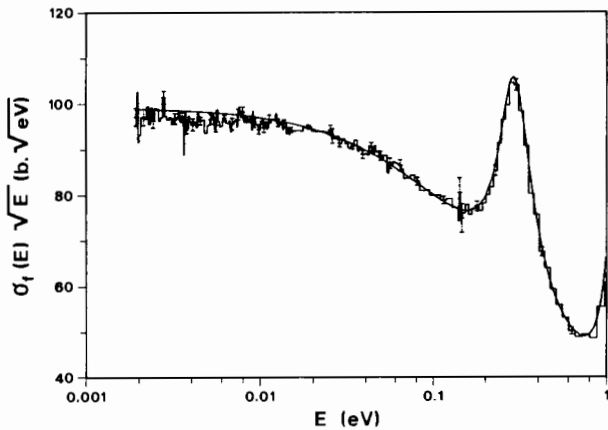


Fig. 6 Measured $\sigma_f(E)\sqrt{E}$ -histogram for ^{235}U . The full line is the ENDF-B5 curve renormalized to $\sigma_f^\circ = 584.25$ b.

Fig. 6 shows the measured $\sigma_f(E)\sqrt{E}$ data for ^{235}U (histogram) in the neutron energy range from 2 meV to 1 eV. The full line is the ENDF-B5 curve (renormalized to $\sigma_f^\circ = 584.25$ b). Within the experimental errors, the experimental data and the evaluated file agree above thermal energy. Below this energy, an agreement exists within two standard deviations although the measured data below 10 meV clearly go faster to a $1/v$ -shape than the evaluated curve. The same tendency is present in the σ_f -data of Deruytter et al.⁷ and Gwin et al.⁹ and in the σ_t -data of Spencer et al.¹⁰. On the other hand, Okazaki and Jones¹¹ reported that integral or effective cross-section measurements in well thermalized neutron spectra of different temperature indicate that the ENDF-B5 shape describes the fission cross-section shape for ^{235}U adequately.

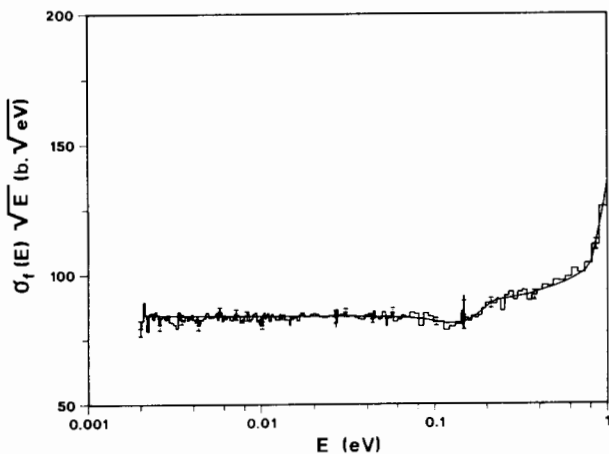


Fig. 7 (above) shows the measured $\sigma_f(E)\sqrt{E}$ data for ^{233}U (histogram) in the neutron energy range from 2 meV to 1 eV. The full line is the ENDF-B4 curve renormalized to the ENDF-B6 σ_f° -value. Both results are in good agreement.

Fig. 8 shows an exploded view of the ^{233}U data in the neutron energy region from 2 meV to 100 meV together with the corresponding results for ^{239}Pu . Also the present ^{239}Pu data agree with the ENDF-B4 curve within the experimental uncertainties, although they tend to be slightly lower below 10 meV.

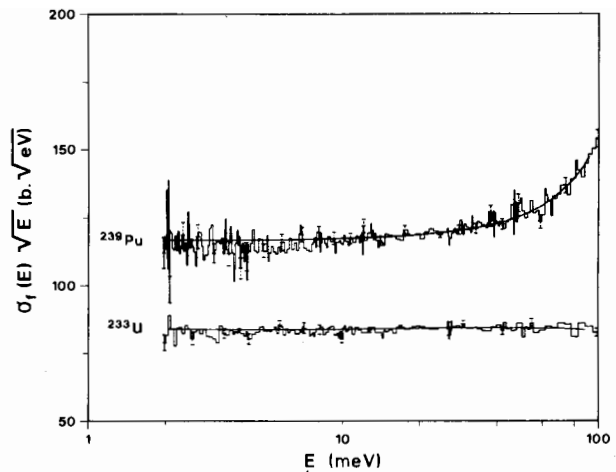


Fig. 8 Measured $\sigma_f(E)\sqrt{E}$ -histograms for ^{233}U and ^{239}Pu . The full lines are the renormalized ENDF-B4 curves.

Fig. 9 (below) shows the $\sigma_f(E)$ -curves in the neutron energy region 1-11 eV for the three isotopes.

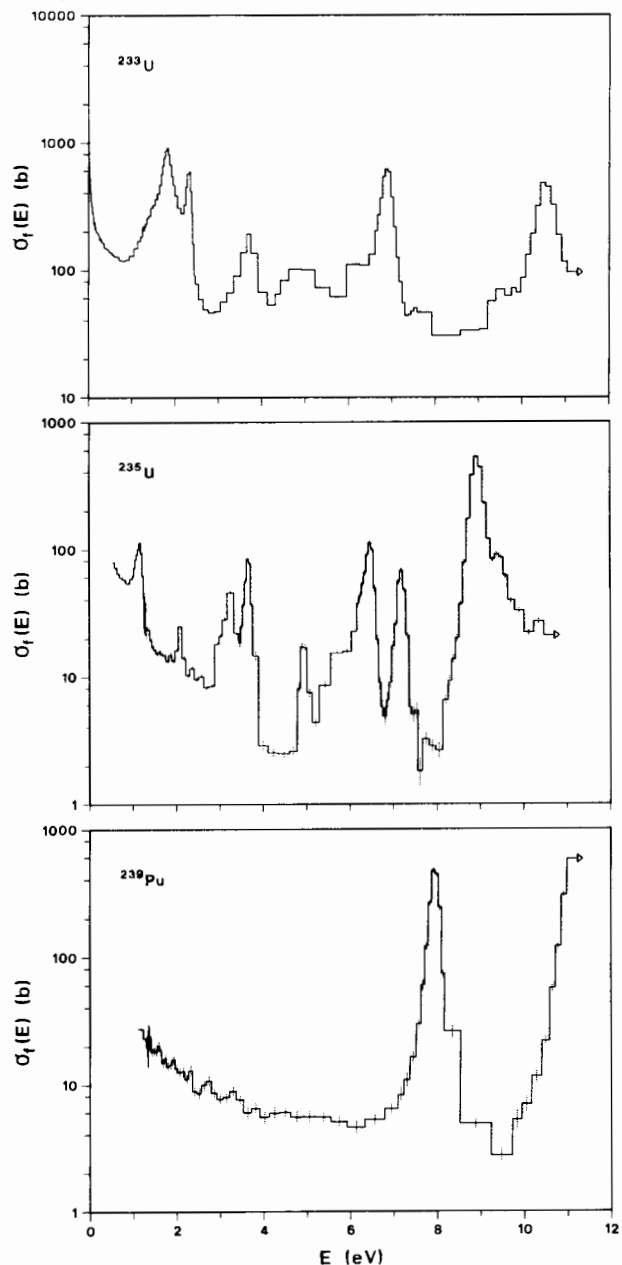


TABLE 1 Fission integrals $\int_{E_1}^{E_2} \sigma_f(E) dE$ (b.eV).

E ₁ (eV)	E ₂ (eV)	²³³ U		²³⁵ U			²³⁹ Pu		
		This work	Deruytter ^{6,a}	This work	Gwin ^{9,b}	ENDF-B5 ^c	This work	Gwin ^{9,d}	ENDF-B5 ^c
0.01	0.02	6.96		7.85	7.85	7.92	9.73	9.79	9.74
0.02	0.10	29.41	29.34	30.57	30.60	30.63	44.93	45.08	44.83
0.10	0.50	70.03	70.23	63.51	63.97	63.96	470.0	465.6	
0.50	1.00	63.70	62.77	30.61	30.70	31.24	39.66	38.49	38.49
1.00	10.00	1248.2	1239.0	370.7	373.4	377.9	252.5	247.2	
8.10	17.60	965.2	964.1						
7.80	11.00			242.5	246.6	(241.5)			
9.00	20.00						1067.6	1067.3	1058.7

a) renormalized to I₁

c) renormalized to σ_f⁰ of ENDF-B6

b) renormalized to I₂

d) renormalized to I₃

Fission integrals

Since these σ_f-measurements were performed under excellent measuring conditions (low repetition frequency, low background, thin samples), they were also used to calculate selected fission integrals. These are summarized in Table 1, which also includes the most recent analogous measurements and the ENDF-B5 values (when available), all renormalized to the σ_f⁰-values from ENDF-B6. This table clearly illustrates that there is a good agreement between the present results and those of Deruytter and Wagemans⁶ for ²³³U and those of Gwin et al.⁹ for ²³⁵U and ²³⁹Pu. Also the renormalized ENDF-B5 values are in fair agreement.

k being the Boltzmann constant, E₀ = 0.025298 eV and T the absolute temperature. The g_f-factor is important for the physics of thermal reactors and is especially useful for the interpretation of measurements done with neutrons having a Maxwellian energy distribution or with a reactor spectrum with a similar shape. The value of g_f is determined by the shape of σ_f(E) below 1 eV. The σ_f data below 20 meV even contribute with roughly 30% to the total g_f-value.

Westcott g_f-factors

Westcott¹² defined the effective cross-section σ̂(T) for neutrons having a pure Maxwellian energy distribution with absolute temperature T as the product of the cross-section at thermal energy σ⁰ and the so-called g-factor:

$$\hat{\sigma}(T) = \sigma^0 g(T)$$

This g-factor is a function of the temperature and can be calculated from the cross-section curve σ(E) in the low energy region via the following expression:

$$g(T) = \frac{1}{\sigma^0 \sqrt{E_0}} \int_0^\infty \sigma(E) \sqrt{E} n(E) dE \quad \text{with}$$

$$n(E) = \frac{2n\sqrt{E}}{(nkT)^{3/2}} \exp \{-E/kT\}$$

$$\text{and } \int_0^\infty n(E) dE = 1$$

Table 2. Westcott g_f-factors at T = 20.44°C

Reference	²³³ U	²³⁵ U	²³⁹ Pu
Hanna (1969)	0.9950 ± 0.0021	0.9766 0.0016	1.0548 ± 0.0030
Steen (1972)	0.9966	-	-
Leonard (76/81)	-	0.9775 ± 0.0011	1.0535 ± 0.0015
Lemmel (75/82)	0.9967 ± 0.0017	0.9762 ± 0.0012	1.0555 ± 0.0024
Divadeenam (1984)	0.9955 ± 0.0015	0.9761 ± 0.0012	1.0558 ± 0.0023
Axton (1986)	0.9955 ± 0.0014	0.9774 ± 0.0008	1.0555 ± 0.0022
ENDF/B 5	0.9966	0.9775	1.0582
ENDF/B 6	0.9955 ± 0.0014	0.9771 ± 0.0008	1.0563 ± 0.0021
Present work	0.994 ± 0.003	0.976 ± 0.002	1.055 ± 0.003

As the available differential data in the neutron energy region $0 \leq E_n \leq 20$ meV are scarce and sometimes discrepant, better data in this region will improve the accuracy of the g_f -factor.

New g_f -calculations were done, making only use of the present fission cross-section results for ^{233}U , ^{235}U and ^{239}Pu . The extrapolation towards zero energy was done by using a least squares fit $\sigma_f \sqrt{E} = a + bE + cE^2$ which was applied to the data points in the energy region from 0.002 eV to 0.1 eV. This extrapolated part contributes only with about 1.5% to the g_f -value (at $T = 20.44^\circ\text{C}$).

The $g_f(T)$ -curves obtained in this way are shown in Fig. 10. The values at $T = 20.44^\circ\text{C}$ are given in Table 2, which includes a series of evaluated values.

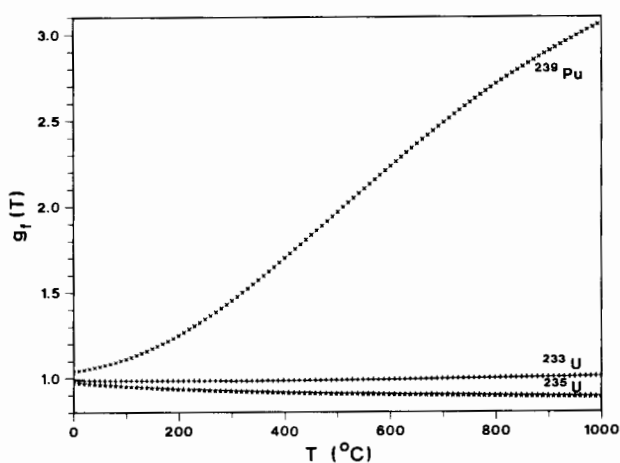


Fig. 10 $g_f(T)$ -curves calculated from the present $\sigma_f(E)$ -data

Conclusion

The present experiments yield new $\sigma_f(E)$ -data for ^{233}U , ^{235}U and ^{239}Pu in the neutron energy region from 0.002 eV to 20 eV. The results for ^{233}U and ^{239}Pu agree with the ENDF-B4 curves renormalized to the same σ_f^0 -values, although the ^{239}Pu data below 10 meV tend to be slightly lower. The present results for ^{235}U agree with the renormalized ENDF-B5 curve above 10 meV. Below that energy they go faster to a $1/v$ -shape.

Also the fission integrals and the Westcott g_f -factors calculated from the present data agree with the most recent experimental and evaluated values.

REFERENCES

1. J. Bouchard, C. Golinelli, H. Tellier, Proc. Int. Conf. on Nuclear Data for Science and Technology (K. Böckhoff ed.), Reidel Publishing Co, 21 (1983).
2. A. Santamarina, C. Golinelli, L. Erradi, ANS Topical Meeting on Reactor Physics, Chicago (1984).
3. C. Wagemans and A. Deruytter, Radiation Effects 93, 163 (1986).
4. C. Bastian, CBNM Geel, Internal Report.
5. A. Carlson, G. Hale, R. Peelle, W. Poenitz, private communication (1987).
6. A. Deruytter and C. Wagemans, Nucl. Sci. Engn. 54, 423 (1974).
7. A. Deruytter, J. Spaepen, P. Pelfer, Journ. of Nucl. En. 27, 645 (1973).
8. A. Deruytter and W. Becker, Ann. of Nucl. Sc. & Engn. 1, 311 (1974) and C. Wagemans, G. Coddens, H. Weigmann, R. Barthélémy, Ann. of Nucl. En. 7, 495 (1980).
9. R. Gwin, R. Spencer, R. Ingle, J. Todd, S. Scoles, Nucl. Sci. Engn. 88, 37 (1984).
10. R. Spencer, J. Harvey, N. Hill, L. Weston, Nucl. Sci. Engn. 96, 318 (1987).
11. A. Okazaki and R. Jones, Radiation Effects 93, 541 (1986).
12. C. Westcott, Journ. of Nucl. En. 2, 9 (1955).